Conf-830607--6

NONLINEAR FLUID/STRUCTURE INTERACTION RELATING A RUPTURE-DISC PRESSURE-RELIEF DEVICE

by
B. J. Hsieh, C. A. Kot, Y. W. Shin, and C. K. Youngdahl
Components Technology Division
Argonne National Laboratory, Argonne, IL

CONF-830607--6

DE83 010737

ABSTRACT

Rupture disc assemblies are used in piping network systems as a pressure-relief device. The reverse-buckling type is chosen for application in a liquid metal fast breeder reactor. When the pressure on the disc is of certain magnitude and history, the disc develops large displacement, is consequently torn open by a cutting-knife setup and thus relieves the excess pressure.

This assembly is used successfully in systems in which the fluid is highly compressible, such as air; the opening up of the disc by the knife setup is complete. However, this is not true for a liquid system; it had been observed experimentally that the disc may open up only partially or not at all. Therefore, to realistically understand and represent a rupture disc assembly in a liquid environment, the fluid-structure interactions between the liquid medium and the disc assembly must be considered.

In this paper, the methods for analyzing the fluid and the disc and the mechanism interconnecting them are presented. The fluid is allowed to cavitate through a column-cavitation model and the disc is allowed to become plastically deformed through the classic Von Mises' yield criteria, when necessary.

NOMENCLATURE

c	Characteristic wave speed in a fluid
$\{D\}$	Nodal displacement vector of a rupture disc
$\{\dot{D}\}$	Nodal velocity vector of a rupture disc
$\{\ddot{D}\}$	Nodal acceleration vector of a rupture disc
$F(u)$	Velocity-dependent pipe friction effect
$\{F^e\}$	Nodal force vector of a rupture disc due to externally applied force
$\{F^r\}$	Nodal force vector of a rupture disc due to induced restoring force
$G(\alpha)$	Pipe-angle-of-inclination-dependent gravity effect
h	Time step of the numerical integration of the equation of motion of a rupture disc
$[M]$	Mass matrix of a rupture disc
p	Pressure at a fluid position; or on a rupture disc
R	Symbolic representation of the equation of motion of a rupture disc

t Time, temporal independent variable

u Velocity at a fluid position

v Average velocity of a rupture disc

x Position, spatial independent variable

ρ Mass density of a fluid

INTRODUCTION

Liquid sodium is used in an LMFBR primary cooling loop or piping network system to transfer the heat generated by the reactor core to the working fluid of the secondary or another loop. To correctly design these loops or piping networks against any possible damage that may be caused by the sudden surge of pressure in the system, an analytical capability to study the transient of pressure waves in piping networks is needed. Through analysis the network's integrity can generally be met by designing the wall of the pipes to be strong enough or thick enough so that under normal and reasonably high pressure situations the pipes will not be stretched to beyond their elastic limit. However, this practice may result in the need to design the pipes to such thickness that they are practically useless either for economic reason or for technical problems such as insufficient space to accommodate these pipes in the plant or from failure due to thermal gradient across the thickness. Two approaches can be used to circumvent these "thick wall" pipe problem: one is to allow the pipe to deform plastically when the pressure is of high but infrequent magnitude such as occurs in an assumed accident, and the other one is to prevent high pressure in the system by dumping the fluid in a tank when some severe situations are detected. An example of the latter is the use of pressure-relief devices.

A pressure relief device is one artificially weakened spot or section of a piping network. At this section or spot, the pipe is weakened by adding to it a device which has a weaker structural strength than the regular pipe. This device is designed to fail or open at a pressure level or pressure history which does not cause any damage to the rest of the piping system. Once this device breaks or opens, it may activate other mechanisms (such as sounding off an alarm and automatic dumping of the fluid in the system) thus protecting the integrity of the rest of the piping system.

The reverse-buckling rupture-disc pressure-relief device is composed of a spherical shell with edge clamped and a cutting knife assembly. The concave side of the disc is always facing the working fluid of the system, and the knife assembly is placed immediately near the shell on the convex side of it [Fig. 1]. Due to the geometry of the disc and the direction of the pressure loading, the disc may become unstable when the pressure loading is above certain magnitude and of certain "frequency content." When this happens, the disc starts large-displacement motion and may be cut open by the knife and effectively reduce the rupture disc to an "open end." In other words, the rupture disc assembly is a time-dependent boundary condition to a piping-network transient analysis.

Thus the response of the structure of the piping network influences the pressure transient in two ways: one through the pipe deformation and the other through special structural type boundary, such as a rupture disc. Since the pressures are high in certain transient accidents, the plastic deformations in the pipes and in the rupture discs must be included when necessary. Therefore a valid and effective pressure transient analysis method must be capable of treating the phenomenon of the interactions between the working fluid and the pipe structures. In other words, this requires a coupled analysis, and the response of the working fluid and the structure must be calculated simultaneously. And to realistically analyze the pressure transient, it is also necessary to include the effect of cavitation of the fluid.

The fluid-structure interaction including the effect of fluid cavitation was reported in [1,2,3,4]. However, in these the rupture disc was treated as a special point boundary without reference in detail as to how the structural response of the disc is obtained. Thus, in this paper using the same fluid-hammer analysis and column separation method, we study the effect of the interaction between the disc and the fluid with particular emphasis on the method of structural analysis for the disc.

FLUID-HAMMER MODEL

The hydraulic transients in the piping system are treated in a standard manner [2,5] by using a one-dimensional fluid-hammer analysis. It is assumed that the axial velocity is the only nonzero velocity component and that the motion in the radial direction is accounted for by the effect of the wall deformation on the wave speed. In general the pipe wall deformation may have both an elastic and a plastic component [3,6,7] resulting in a variable wave speed in the pipe.

When expressed in terms of dependent variables p (pressure) and u (velocity) the equations governing fluid transients can be written in characteristic form as follows [2,4]:

Along positive characteristic

$$\frac{dx}{dt} = u + c \tag{1}$$

$$\frac{du}{dt} + \frac{1}{\rho c}\frac{dp}{dt} + F(u) - G(\alpha) = 0 \tag{2}$$

Along negative characteristic

$$\frac{dx}{dt} = u - c \tag{3}$$

$$\frac{du}{dt} - \frac{1}{\rho c}\frac{dp}{dt} + F(u) - G(\alpha) = 0 \tag{4}$$

Here x and t are the space and time coordinate, respective, ρ is the density, c is the wave speed, F(u) is the velocity dependent pipe friction effect, and $G(\alpha)$ represents the effect of gravity when α is the angle of pipe with the horizon.

The wave speed c for the pipes that are deformed elastically or elastoplastically are explicitly given in [1,3,6,7].

COLUMN-SEPARATION MODEL

The treatment of transient cavitation is based on a generalization of the basic column-separation technique. In this approach, cavitation is a local phenomenon which occurs wherever the pressure drops below the vapor pressure. The cavity is assumed to remain at the constant vapor pressure and forms a free boundary for the separated fluid columns. Cavitation is assumed to cease when the cavity vanishes by reimpact of adjacent fluid columns or of a fluid column and a structural boundary.

To accommodate the phenomenon of column separation, two values of velocity are introduced at each point. If no cavitation exists, the two velocities at the point are equal, and one obtains the solution by solving the characteristics relationships (2) and (4) for the pressure and velocity.

Cavitation is assumed to occur when the pressure predicted by eqs. (2)-(4) falls below the vapor pressure, p_{vap}, corresponding to the prevailing fluid temperature. When this occurs, the pressure at the point is set to p_{vap} and the two velocities are, respectively, obtained by substituting this pressure into the appropriate characteristic equations, eqs. (2) and (4). The size of the cavity at this point is computed by integrating the difference of velocities at this point with respective to time. The cavity at a point is assumed to have collapsed when the size of cavitation thus computed is nonpositive. Note that during sudden expansion of a fluid, the fluid pressure may significantly undershoot the vapor pressure corresponding to the fluid temperature. Such phenomena have been observed to occur during rapid depressurization of water; however, they are not expected in the liquid sodium environment. Therefore, the column-separation model is expected and works well in a sodium environment. The undershooting in the water environment can be incorporated into the column-separation model if the characteristics of the undershooting of pressure as a function of the speed of cavitation is known.

The details of the procedures for treating the cavitation of the fluid are available in [1].

RUPTURE-DISC/FLUID MODEL

Any interior point of a pipe has two characteristics equations to be satisfied, given by eqs. (1)-(4), when there is no cavitation at the point. If cavitation has been noted to occur, then the solution is obtained by setting the pressure to the vapor pressure in the characteristics equations. That is, for an interior point, the solution, i.e., pressure and velocity, can be obtained by solving the two characteristics equation for the two unknowns or by solving the two equations with an imposed condition that the pressure is p_{vap} and resulting in two velocities at a cavitated point. At any end point of a pipe, however, the situation is different, because of the nonexistence of a characteristics equation representing the propagation of the disturbance into the nonexistent fluid. Thus, there is only one characteristics equation available at an end point to provide a solution for the pressure and velocity; the other condition for a unique determination of the solution is given by the specific boundary condition on either the pressure or the velocity. Many different and useful boundary conditions, such as surge tank, open end, or closed end, were defined in this manner [7].

The rupture-disc boundary condition is a natural extension of the above-explained boundary condition, i.e. the pressure and the velocity are to be determined by a characteristics equation and an additionally specified condition. The difference between this and the other boundaries is that the condition is given through a highly nonlinear relationship between the pressure and the velocity. That is, the pressure and velocity at a rupture disc must also satisfy

$$\dot{v} = R(p) \tag{5}$$

in addition to the equation associated with the fluid or cavitation characteristics equation. Here v is the velocity and p is the pressure of the disc. The velocity and pressure at the disc may or may not be the same as that of the fluid, depending on whether cavitation has occurred. The relationship R usually is not known explicitly, but its effect can be modeled through the numerical integration of a discrete finite-element model of the disc. The approach to model R is the topic to be described below.

FINITE-ELEMENT MODEL OF A RUPTURE DISC

A rupture disc subjected to a pressure applied over its concave side has the potential of becoming unstable when the pressure is of a certain shape and magnitude. Without resorting to numerical techniques, there appears to be no analytical method which can treat this phenomenon and provide a useful quantitative solution. Hence, numerical methods seem highly attractive, particularly when the nonlinearity due to material properties is also of potential importance, in addition to that caused by the geometry of the disc.

The finite-element method is used in this analysis to generate a mathematical model providing the necessary relationship R. This is a model which produces the required velocity v from a given time history of pressure p. The details for this finite-element formulation are available in [8,9]; therefore only the essence of this method is briefed here.

Though the process may be lengthy the conventional formulation of the finite-element method can be applied in a straight-forward manner to represent a rupture disc, by breaking up the disc into a finite number of subregions or elements and utilizing the principle of virtual work over the assembly of the elements. Because the distribution of the displacement within each element is assumed to be a known function of the displacements at the nodes of the elment, called nodal displacements, the approach results in differential equations in terms of the nodal displacements. These equations can then be integrated in time in a step-by-step manner.

Unfortunately, for rupture disc applications where the displacement may not be small, the use of the conventional approach requires a high-order shape function for the displacement distribution in an element and complicated constitutive relations. However, accuracy is improved and computational cost is reduced when a particular coordinate system, convective or corotational system, is used without using high-order elements, etc. This is a method in which the shape functions are assumed in terms of a coordinate system that rotates and translates but does not deform with an element. Thus, a displacement that cannot be separated into additive rigid-body-motion and deformation components in terms of the global coordinates system can be so separated in the corotational coordinates. This makes the corotational finite-element method very attractive for problems where displacements are large but the strains may be small [10]. The behavior of a rupture disc belongs to this type of behavior.

The equation of motion for a rupture disc can be written as

$$[M]\{\ddot{D}\} = \{F^e\} - \{F^r\} \tag{6}$$

where [M] is the mass matrix, {D} the nodal displacement vector (a superscript dot means time derivative), $\{F^e\}$ the externally applied nodal force vector which depends on the pressure distribution p on the disc and $\{F^r\}$ the induced internal restoring force vector. The dimension of these matrix and vectors is a function of the number of elements of the model, and [M], $\{F^e\}$, and $\{F^r\}$ can be computed from the formulas derived in [8,10]. Numerical parameter study may and should be performed to determine an optimum number of elements for each specific rupture disc.

Since the number of elements usually is much greater than one, the finite element modeling for the rupture disc is truly two-dimensional. In other words the pressure and velocity distributions of the disc are not uniform in terms of the space variable. To interact the disc model and the one-dimensional fluid-hammer model, one must, therefore, artificially define a pressure distribution of the disc for input to the finite-element model and an average velocity of the disc to return to the fluid-hammer model as an output. The pressure distribution assumed is a uniform one and the average velocity defined is the change of volume swept by the disc in unit time divided by its base area. Thus the disc model, eq. (6), provides an implicit relationship for R of eq. (5). The validity of this finite-element model was shown in [8,9].

Equation (6) is integrated in time by the explicit central-difference technique

$$\begin{aligned} \{\dot{D}(t+h)\} &= \{\dot{D}(t)\} + \frac{h}{2}\left(\{\ddot{D}(t)\} + \{\ddot{D}(t+h)\}\right) \\ \{D(t+h)\} &= \{D(t)\} + h\,\{\dot{D}(t)\} + \frac{1}{2}(h)^2\,\{\ddot{D}(t)\} \end{aligned} \tag{7}$$

where h is the time step of the numerical integration. The magnitude of h must be small so that numerical stability is conserved. This is not a problem, since h must be small for accuracy in certain "path-dependent" constitutive laws, such as in a plasticity law. Because of the smallness of h for a disc compared to the time step needed to integrate eqs. (2) and (4), tens or hundreds of h's are needed for each fluid step. The pressure p on the disc must be appropriately interpolated in time from the fluid-hammer equation to warrant the convergency of solution of the interaction between the disc and the fluid. The details of this are available in [1].

INTERACTIONS BETWEEN A FLUID AND A RUPTURE DISC

The rupture disc of reverse buckling type [see Fig. 1] is used in certain designs of piping networks to provide pressure relief when accidents occur. The disc is designed to have only nominal motion when the pressure it receives is "subbuckling" and to buckle quickly or snap through when the pressure is significant. The snap through of a rupture disc is a dynamic process, and it is hoped that the disc will be completely torn open by the cutting knife setup placed immediately behind it, thus dumping the fluid in the pipe. Indeed, this is the case when the working fluid is a gas; this is supported by the successful use of reverse buckling rupture discs in gas environments in the chemical industry. However, this may not be the case when the working fluid is liquid. For example, it had been experimentally observed that a disc may just rest on the cutting knife without being torn open for certain loading conditions in a water filled pipe [11]. This phenomenon is attributed to the near incompressibility of a liquid compared to that of a gas. To visualize this, consider a fluid-filled pipe with one end of the pipe being a rupture disc and the other being a closed end. Suppose the fluid is being pressurized to certain levels while the potential motion of the disc is suppressed by some means. If one now removes the constraint on the disc, the disc will start to move away from the fluid at least for the early stage, independent of the nature of the fluid; however, the pressure history or the loading on the disc is quite different for later time for different fluids. For example, if the fluid is gas, which is highly compressible (i.e., large volume change of the gas corresponds to small change of the pressure and vice versa), then the pressure on the disc is effectively constant in time. On the other hand, if the fluid is a highly incompressible liquid, such as water or sodium, a small movement of the disc reduces drastically the pressure on the disc; hence the pressure on the disc is not constant but decaying in time. Consequently, had the pressure of the fluid been greater than the static snap-through or buckling pressure of the disc, the disc would have buckled in the case of gaseous fluid, but might not have in the liquid case.

Note that a pressure reduction is expected once the disc starts moving away from the liquid. This reduction of pressure is a function of the properties of the disc, the fluid and also of the pressure and velocity of the liquid, i.e., the transient in the liquid. The reduction of pressure is important because it provides the physics as to why the disc may just rest on the knife without being open in a liquid system, since a reduction of pressure effectively reduce the momentum carried by the disc. Therefore, any valid and effective fluid-structure interaction analysis must be able to predict such reduction of pressure.

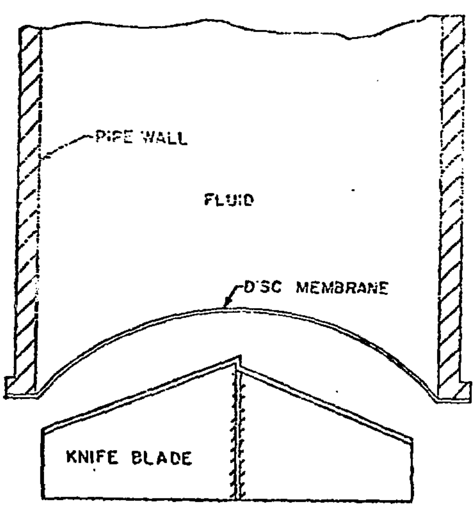

Fig. 1 Reverse Buckling Rupture Disc Design

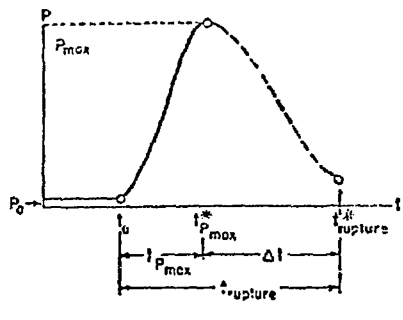

Note: (1) Disc loading rate is computed as $(P_{max}-P_o)/t_{P_{max}}$

(2) Failure time, $t_{rupture}$, is defined as when disc reached 1.875"

Fig. 2 Typical Pressure History on a Disc

Through the use of a model of a liquid-filled pipe with one end treated as a rupture disc and the other a pressure source with linearly increasing pressure histories, many numerical results were obtained and examined. To concentrate on the interaction phenomena, only responses of the disc are presented. A typical pressure history on a disc is given in Fig. 2, where P_o is the initial system pressure of the pipe, P_{max} is the maximum pressure experienced by the disc, and t_a is the time the source pressure first arrives at the disc. Due to the huge demand on computer resource and due to the lack of details to treat the tearing process in a quantitative way, the computation for the disc response is terminated when the disc reaches* the knife. Afterwards, the disc is considered as an open end, i.e., for $t > t_{rupture}$.

It should be noted that since the pressure is monotonically increasing until P_{max} is reached, a loading rate on the disc can be computed by using $(P_{max} - P_o)/t_{max}$. A summary of the pressure on a disc for various source loading rates is shown in Table 1. The entries for the columns are explained in Fig. 2. Note that the length of pipe for the first two runs is different than that of the other runs, as indicated by the values for t_a in the fifth column. From Fig. 2, one sees that the maximum pressure of the disc is by definition occurring right before the occurrence of the reduction of pressure due to disc movement. In other words, one can say that the maximum pressure is the pressure at which significantly large motion of the disc starts to occur. This leads to the observation that P_{max} can be considered as the "dynamic buckling pressure" of the disc subjected to linearly increasing loadings and that the static buckling loading may be obtained by back extrapolating the results to zero loading rate.

Table 1. Effect of Loading Rate

(1) Source Loading rate, ksi/s	(2) P_{max} psi	(3) $t^*_{P_{max}}$ ms	(4) $t^*_{rupture}$ ms	(5) t_a ms	(6) $t_{P_{max}}$ ms	(7) $t_{rupture}$ ms	(8) Disc Loading rate, ksi/s	(9) Disc Rate / Source rate	(10) Δt ms
5	485	94.6	93.0	46.7	47.9	52.3	9.818	1.964	4.4
10	491	71.4	75.4	46.7	24.7	28.7	19.283	1.928	4.0
20	501	36.0	39.7	23.1	12.9	16.6	37.658	1.883	3.7
40	522	30.2	33.2	23.1	7.1	10.1	71.452	1.786	3.0
60	539	28.2	30.9	23.1	5.1	7.8	102.804	1.713	2.7
80	555	27.2	29.7	23.1	4.1	6.6	131.780	1.647	2.5
100	577	26.8	28.9	23.1	3.7	5.8	151.973	1.520	2.1

From column two of Table 1, it is clear that the dynamic buckling loading for the disc increases as the source or disc loading rate is increased. Also noted from column six is that it takes a longer time for the pressure to build up for the lower loading rate cases and from column 9 that the ratio of the disc loading rate to source loading rate decreases from a value of two as the loading rate increases. It is not difficult to understand that the ratio should reduce to zero if a step loading is applied as a source pressure. This means that it is not possible to effectively apply a step loading on the disc, due to the interactions between the liquid and the disc. This also means that before the disc buckles it can be treated more like a closed end at low loading rate than at higher ones. This is because the loading rate ratio is two at a closed end according to the acoustic theory, and the deviation from this value indicates the movement of the disc away or toward the fluid. The reduction of the value from two at higher loading rate thus indicate that the disc moves away from the fluid. The last column shows the time lapse between the instant the disc starts to move to the instant it reaches some specified value, i.e., it reaches the knife. In other words, it is the time the disc needs to travel across a known distance; therefore the values in the last column reflect the momenta carried by the disc when buckling occurred. It thus can be concluded that the disc is more likely to be torn open when subjected to higher loading rates.

Various plots for the entries of the column were plotted to show the effect of loading rate; however, to save space only the maximum pressure entry is shown in Fig. 3. As mentioned earlier, the static buckling pressure can be extrapolated from this figure and was found to be about 3.32 MPa (482 psi). Compared to the buckling pressure of 3.34 MPa (485 psi) for the loading rate of 34.47 MPa/s (5 ksi/s), it is concluded that this loading rate is slow enough to represent a static loading condition for the disc/fluid system.

The static buckling pressure of the discs used in this example has a nominal buckling pressure of 2.24 MPa (325 psi) with an error not to exceed 5% of the nominal value. Nontheless the computed value for an elastic disc is

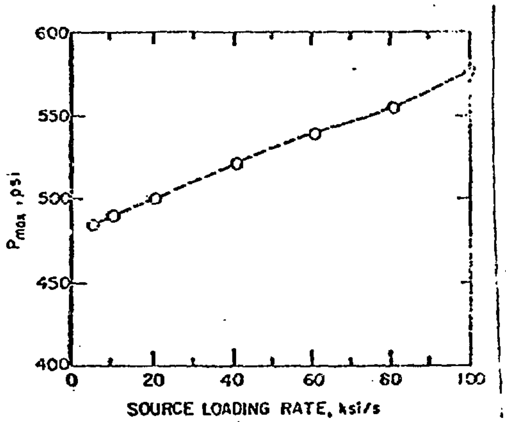

Fig. 3 Effect of Yield Stress on Static P_{max}

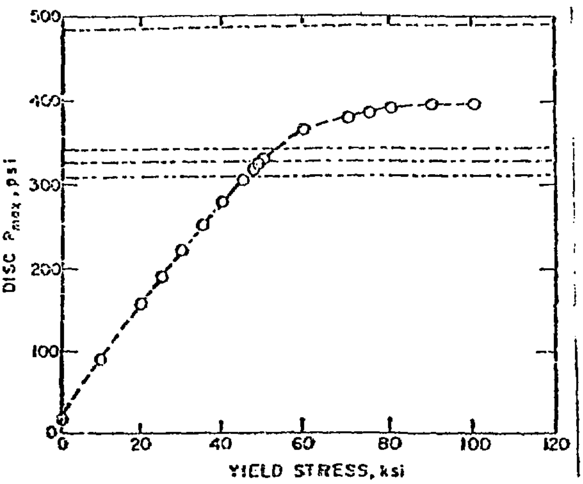

Fig. 4 Effect of Source Loading Rate on P_{max} (Dashed line: elastic solution; Dashed-dotted line: nominal value and 5% tolerance)

3.34 MPa (485 psi) or a discrepancy of 50%. To understand this discrepancy, an elastoplastic constitutive model with von Mises' yield criteria and associated flow rules that has a tri-linear stress-strain relation is used to examine the effect of plastic deformation of the disc [10]. The "static loading rate" of 34.47 MPa/s (5 ksi/s) just established was used for the source loading. Parameter studies were performed for the plastic model. For example, the effect of the yield stress on the pressure of the disc is summarized in Table 2. Note that, though the maximum pressure and its occurrence time are monotonically increasing functions of the yield stress, the momentum carried by the disc (reflected by Δt in the last column) is not. There appears to be a drastic change in momentum when the yield stress reaches 275.79 MPa (40 ksi). One possible explanation of this phenomenon is that for low yield stress, the disc may develop more plastic strains or hinges, thus forming a mechanism; while the high yield stress one may still be almost elastic. Because of the mechanism of the "plastic hinges," the "plastic" one is expected to move faster than the elastic one when both are subjected to the same pressure; however, it should be noted that the faster a disc moves, the faster it relieves the pressure exerted on it. Consequently, the exact reason can not be quantitatively identified for this sudden change of disc momentum at a particular yield stress.

Figure 4 shows the static P_{max} obtained for various yield stress when the disc is subjected to a "static" source loading. The top dashed line stands for the buckling pressure for the elastic disc and the three dashed-dotted lines stand for the nominal value and its manufactoring tolerance of the disc. It is thus clear that the static buckling pressure is within the tolerance if the yield stress for the disc is chosen to lie between 310 to 380 MPa (45 to 55 ksi).

CONCLUSION

The fluid-structure interaction analysis including the effect of cavitation was successfully performed for the case of a rupture disc subjected to a linear source loading. The qualitative behavior of the pressure reduction for a liquid system due to disc motion is demonstrated in every numerical example. This provides the explanation for the lack of momentum of the disc to be torn open by the knife under certain loading conditions in a liquid system. It was also demonstrated that, by appropriately choosing the yield stress and source loading rate, the static buckling pressure of the disc can be computed to within the manufacturer's specified tolerance.

However, the rupture disc assembly is transformed into an open end once the disc reaches the knife. To follow the motion of the disc after its contact

However, the rupture disc assembly is transformed into an open end once the disc reaches the knife. To follow the motion of the disc after its contact with the knife requires more computational resources and mechanical knowledge of the tearing process, particularly when asymmetric deformation is of importance. More research is needed in this area.

Table 2. Effect of Yield Stress for a Loading Rate of 5 ksi/s

σ_y ksi	P_{max} psi	$t^*_{P_{max}}$ ms	$t^*_{rupture}$ ms	t_a ms	$t_{P_{max}}$ ms	$t_{rupture}$ ms	Δt ms
∞	455	94.6	99.0	46.7	47.9	52.3	4.4
100	394	85.6	90.6	46.7	38.9	43.9	5.0
90	393	85.4	90.4	46.7	38.7	43.7	5.0
80	389	85.0	89.9	46.7	38.3	43.2	4.9
75	386	84.6	89.4	46.7	37.9	42.7	4.8
70	378	86.0	88.8	46.7	37.3	42.1	4.8
60	364	[illegible]	87.6	46.7	35.9	40.7	4.8
50	328	79.2	84.2	46.7	32.5	37.5	5.0
49	323	78.6	83.9	46.7	31.9	37.2	5.3
45	319	78.2	83.5	46.7	31.5	36.8	5.3
45	303	76.8	82.3	46.7	30.1	35.6	5.5
40	280	74.4	80.5	46.7	27.9	33.8	5.9
35	251	71.3	96.3	46.7	25.1	49.6	24.5
30	222	68.3	94.6	46.7	22.1	47.9	25.8
25	193	65.6	93.0	46.7	18.9	46.3	27.4
20	158	62.4	91.5	46.7	15.7	44.8	29.1
10	90	55.8	89.7	46.7	9.1	42.0	32.9
0	55.44	53.0	82.4	46.7	6.3	35.7	29.4

ACKNOWLEDGMENTS

This work is supported by the U. S. Department of Energy.

REFERENCE

1. Kot, C. A., Hsieh, B. J., Youngdahl, C. K., and Valentin, R. A., "Transient Cavitation in Fluid-Structure Interactions," Journal of Pressure Vessel Technology, Vol. 103 Nov 1981.
2. Kot, C. A. and Youngdahl, C. K., "Transient Cavitation Effects in Fluid Piping Systems," Nuclear Engineering and Design, Vol. 45, No. 1, Jan. 1978, pp. 93-100.
3. Youngdahl, C. K., Kot, C. A., and Valentin, R. A., "Pressure Transient Analysis in Piping Systems Including the Effects of Plastic Deformation and Cavitation," ASME/CSME Pressure Vessel and Piping Conference, Paper No. 78-PVP-56, Montreal, Canada, June 25-30, 1978.
4. Kot, C. A. and Youngdahl, C. K., "The Analysis of Fluid Transients in Piping Systems, Including the Effects of Cavitation," Symposium on Fluid Transients and Acoustics in the Power Industry, ASME Winter Annual Meeting, San Francisco, Calif., December 10-15, 1978.
5. Streeter, V. L., and Willie, E. G., Hydraulic Transients, McGraw-Hill, New York, 1967.
6. Youngdahl, C. K. and Kot, C. A., "Effect of Plastic Deformation of Piping on Fluid-Transient Propagation," Nuclear Engineering and Design, Vol. 35, 1975, pp. 315-325.
7. Youngdahl, C. K. and Kot, C. A., "Computing the Effect of Plastic Deformation of Piping on Pressure Transient Propagation," Computational Methods for Fluid-Structure Interaction Problems, AMD-Vol. 26, ASME Winter Annual Meeting, Atlanta, Ga., November 27-December 2, 1977.
8. Hsieh, B. J., and Belytschko, T. B., "Nonlinear Transient Finite Element Analysis with Convected Coordinates," International Journal of Numerical Method in Engineering, Vol. 7, No. 3, 1973.

9. Hsieh, B. J., "Dynamic Instability Analysis of Axisymmetric Shells by Finite Element Method with Convective Coordinates," 4th International Conference on Structural Mechanics in Reactor Technology, San Francisco, California, August 1977.

10. Hsieh, B. J., "Nonlinear Transient Finite Element Analysis with Convected Coordinates," Ph.D. Thesis, Department of Materials Engineering, University of Illinois, 1974.

11. Reynolds, R. G., "Development Status of Sodium-Water Reaction Pressure Release Rupture Disc for the CRBRP," General Electric Company Report GEFR-00361, UC-79A, July 1978.